Journal of Trace Elements in Medicine and Biology xxx (2018) xxx-xxx

Contents lists available at ScienceDirect

Journal of Trace Elements in Medicine and Biology

journal homepage: www.elsevier.com

Evaluation of the uptake, storage and cell effects of nano-iron in enterocyte-like cell models

Daniel Turiel Fernández, Jörg Bettmer, Maria Montes-Bayón*

Department of Physical and Analytical Chemistry, Faculty of Chemistry, University of Oviedo, C/ Julián Clavería 8, 33006 Oviedo, Spain

ARTICLE INFO

Keywords:
Fe nanocompounds
ICP-MS
Uptake
Cytosol distribution
Ferritin

ABSTRACT

The therapy with nanocompounds is widely used to treat Fe deficiency and an emerging trend to inhibit tumor growth. The present work aims to address the management of different FeONP, comparing sucrose covered FeONP and Fe nanoparticles in the form of the ferritin with non-particulated inorganic Fe (II) by enterocytes-like colon cancer cell lines (Caco-2 and HT-29). Iron uptake results revealed significantly higher Fe incorporation in the case of nanoparticulated Fe, first in the form of FeONP and second in the form of ferritin with respect to inorganic Fe (II). Furthermore, the intracellular Fe fractionation, conducted by size exclusion chromatography coupled on line to inductively coupled plasma mass spectrometry (SEC-ICP-MS) showed a significant increase of the Fe-ferritin peak upon exposure of cells to the following compounds ferritin > FeONP > $FeSO_4$. Such results point out that the sucrose coated FeONP released Fe into the cell cytosol that was used to replenish the existing cytosolic ferritin without inducing changes in the protein concentration. On the other hand, the increase of the Fe-ferritin peak in cells exposed to ferritin as iron source is due to a significant increase on the intracellular protein concentration, as proved by using an ICP-MS linked ferritin sandwich immune assay. Cell viability experiments conducted with concentrations up to 1000 μmol L^{-1} (as Fe) of each compound under scrutiny did not reveal significant differences among Fe species regarding global cellular toxicity. However, significant cell DNA damage was detected when treating the cells with FeONP (500 μmol L^{-1}).

1. Introduction

Iron deficiency anemia (IDA) results from an unbalanced iron absorption, transport and storage in the human body. For management of IDA, oral iron supplementation is normally recommended, if inflammatory or blood loss processes are not occurring [1,2]. Simple ferrous iron Fe(II) salts are most commonly used for this aim since they are inexpensive and the iron is well absorbed. However, recently, these compounds have been found responsible to induce undesirable changes to bacteria of the colon and to increase pro-inflammatory signaling of the gut epithelium enhancing systemic infection rates [3]. As alternative, some forms of ferric iron Fe(III) (e.g. ferric pyrophosphate) have been proposed to be potentially better tolerated in the gut lumen than Fe(II). Unfortunately, they are poorly absorbed by the intestine [4]. To improve the low tolerability and poor bioavailability of ionic Fe species, different approaches have been taken [5]. In particular, Fe from nanocompounds have shown to be more efficiently absorbed than the ionic metal species in animal models without any detectable accumulation in the gastrointestinal tract or other tissues [6].

In fact, the use of iron oxide/hydroxide nanoparticles (FeONP) covered with carbohydrate shells present an interesting alternative for iron supplementation. They are currently indicated in cases of intolerance or inadequate response to oral Fe and administrated as intravenous formulations [7],8]. Nevertheless, some doubts still remain regarding the bioavailability of some of these formulations since their expected diffusion into the enterocytes seems to be not very effective. A way to overcome the limited enterocyte uptake of the Fe-containing nanocompounds is the modification of the NPs surface with specific ligands in order to achieve receptor mediated NPs endocytosis. For this aim, ferritin could be an ideal candidate [9]. Ferritin is an iron-binding protein with very high capacity to store Fe; up to 4500 atoms of Fe can be accumulated in each molecule. It is composed by a protein cage in which Fe is stored in the form of ferrihydrite (poly oxohydroxide Fe(III) nanoparticles). Ferritin is an effective and bioavailable form of dietary iron that has led to considerable interest for its potential use in "bio-

* Corresponding author.
Email address: montesmaria@uniovi.es (M. Montes-Bayón)

https://doi.org/10.1016/j.jtemb.2018.05.002
Received 18 January 2018; Received in revised form 8 April 2018; Accepted 2 May 2018
Available online xxx
0946-672/

fortification" of food crops [10]. Recent experiments in enterocyte-like cells like Caco-2 strongly suggest that ferritin is taken up by enterocytes via receptor-mediated endocytosis. The authors also suggest that macropinocytosis, a secondary mechanism, might be activated at high ferritin concentrations [11]. The capture of ferritin was originally demonstrated in intestine [12], but also in white matter, lymphoid cells, erythroid precursors, in the capsule of the adult kidney etc. In all of these cell types, ferritin used an endocytic pathway and delivered iron to the cytoplasm [13].

The second approach to enhance the uptake of nanocompounds by enterocytes could be the use of Fe-NPs which contain a charged shell. Studies on the effect of charge density and of the kind of charge (positive, negative) in non-phagocytic cells showed that charged iron oxide particles are taken up better than their uncharged counterparts [14]. Although the 'average' charges on the cell surface are negative, the cell membrane also presents specific binding sites with cationic receptors that allow interaction with anionic NPs, in a process described as an "adsorptive endocytosis" pathway [15]. In this regard, Fe(III)-sucrose complex (Venofer®) contains an Fe(III) core surrounded by sucrose that provides a negative charge on the NPs outer shell. This complex is commonly used in intravenous iron formulations and has provided lower anaphylactic reactions in patients that soon after administration recover the adequate iron values in circulating blood [16]. Thus, the aim of this work is the comparative evaluation of these two types of FeONPs (sucrose coated and ferritin encapsulated) regarding enterocytes uptake and management. Thus, the Fe cellular uptake, cytosolic Fe distribution and management as well as Fe-induced cell toxicity will be addressed in enterocyte-like cell models (Caco-2 and HT-29) with respect to iron (II) salts.

2. Experimental

2.1. Instrumentation

Two different ICP-MS instruments were used for this study: an Agilent Instrument 7700 (Agilent Technologies, Tokyo, Japan) and an iCAPTQ ICP-MS (Thermo Fisher Scientific, Bremen, Germany) both with H_2 as collision gas to eliminate polyatomic interferences. The iCAPTQ ICP-MS was also used for Ru determination (ferritin analysis) using the single quadrupole (SQ) mode. For the flow injection set-up, the solvent was pumped using a peristaltic pump ($0.5\,mL\,min^{-1}$) and the sample injection was conducted using dual mode injection valve from Rheodyne, model 9725 (Upchurch Scientific, Oak Harbor, Washington, USA).

For iron speciation in the cellular lysate, size exclusion chromatography (SEC) was used. The mobile phase was pumped using a dual-piston liquid chromatographic pump (Shimadzu LC-20AD, Shimadzu Corporation, Kyoto, Japan) equipped with a sample injection valve from Rheodyne, fitted with a 20 μL injection loop and a size exclusion chromatography column Superdex 200 10/300 GL (300 mm × 10 mm i.d., GE Healthcare Bio-Sciences, Sweden) having a fractionation range from 10 to 600 kDa. The mobile phase flow rate was $0.7\,mL\,min^{-1}$. On line coupling of the HPLC to the Vis/UV detectors was conducted by two different Agilent instruments (Agilent Technologies, Tokyo, Japan) 1100 and 1260 Series monitored at 280 nm and 380 nm using a Diode Array Detector (DAD) detector (Agilent Technologies, Tokyo, Japan).

HR-TEM measurements were done in a JEOL-JEM 2100F (Tokyo, Japan) transmission electron microscope with TEM operation voltage at 200 kV to image iron NPs suspensions deposited on Cu grids. The instrument permits also to obtain the elemental composition of the sample.

2.2. Chemicals and materials

All working solutions were prepared using $18\,M\Omega\,cm^{-1}$ de-ionized water obtained from a Milli-Q system (Millipore, Bedford, MA, USA). The iron ICP-MS standard was purchased from Merck (Darmstadt, Germany) and Ru ICP standard was obtained from Alfa Aesar (Alfa Aesar, Karlsruhe, Germany). Ferritin standard from equine spleen were purchased from Sigma-Aldrich (St. Louis, MO, USA). For the ferritin ICP-MS linked immunoassay, biotinylated anti-ferritin mouse monoclonal antibody ($3\,mg\,L^{-1}$), labeled $[Ru(bpy)_3]^{2+}$ anti-ferritin mouse monoclonal antibody ($6\,mg\,L^{-1}$) and streptavidin covered magnetic microparticles ($0.72\,mg\,mL^{-1}$) (Roche Diagnostics GmbH, Mannheim, Germany) were used. Standard Venofer® solution was kindly provided by the Hematology Group of the Hospital Central Universitario de Asturias (Oviedo, Spain) in the form of an aqueous complex of polynuclear iron (III)-hydroxide in sucrose containing 20 mg elemental Fe per mL. Upon reception, the content of the vial (5 mL) was separated into aliquots of 1 mL and stored at −4 °C until further use. Successive dilutions of the parenteral solution were conducted in 0.9% NaCl, as stated by the manufacturer. $FeSO_4{\cdot}7\,H_2O$ used were purchased from Sigma-Aldrich. SEC separation was done using a mobile phase containing $50\,mmol\,L^{-1}$ ammonium acetate (Merck), pH = 7.4 at $0.7\,mL\,min^{-1}$.

2.3. Cell culture and lysis

The human colorectal adenocarcinoma cell lines (HT29 and Caco-2 cells) were obtained from the Biotechnological and Biomedical Assays in the Technical Services of the University of Oviedo. Cells were grown in T-25 flasks with IMEM medium (LabClinic) and supplemented with 9% FBS (Gibco, Life Technologies, Madrid, Spain) at 37 °C in a 5% CO_2 atmosphere. Then, the cells were washed with $10\,mmol\,L^{-1}$ PBS (pH = 7.4, three times to remove any iron traces from the growing media) and then trypsinized. Cells were placed in six well plates. The number of cells in the case of HT-29 ranged $0.8–1.0\times10^6$ and $0.5–0.6\times10^6$ in the case of the Caco-2 counted using a Neubauer chamber. After 24 h, the different Fe-containing compounds were added. The compounds were added using a syringe filter with 0.2 μm Supor® sterile membrane in order to avoid bacterial contamination. Cells were harvested after 48 h. The quantitative results have been referenced to the wet weight of cells [17]. This was done by washing the cells three times with PBS, removing the supernatant by centrifugation and finally weighting the cell pellet using a precision balance.

Washed cells were lysed using three cycles of freezing/thawing using liquid nitrogen. Then, the cellular lysate was centrifuged ($12{,}000\,g\times20$ min) and the supernatant was collected for further analysis.

2.4. Total cellular iron and Fe speciation

An aliquot of the cell lysate previously acidified with 0.1% HNO_3 was taken for total Fe determination by ICP-MS obtained by continuous nebulization after optimizing the sample consumption. The results were obtained for six independent cell cultures. The Fe uptake, within each cell line, was determined using paired Student *t* tests to compare treatments with negative controls, and linear regression analyses to study whether the response increased with concentration.

A second aliquot of the lysate was used for ferritin determination which will be described in the following section. Additionally, an aliquot of that was also injected into the SEC-ICP-MS and SEC-Vis/UV for Fe speciation experiments.

2.5. Sandwich immunoassay with Ru detection for ferritin determination

Aliquots of 50 μL of independent cell lysates (corresponding to six different cell cultures) were mixed with the biotinylated ferritin-specific antibody and the Ru-labeled ferritin-specific antibody to form a sandwich complex as described elsewhere [18]. The signal of Ru was transformed into ferritin concentration and the values plotted as the mean with error bars corresponding to the standard deviation to compare treatments with control.

2.6. Comet assay

This assay is used in order to detect the presence of DNA strand breaks in HT-29 cells. After the incubations, we diluted the cells to obtain 650 cells per sample holder and carried out the assay as described by Sar et al. [19]. Cells were visualized at 400 times magnification with an Olympus DP-70 CCD-coupled camera (from the Scientific and Technical Services of the University). The photos were analyzed with the Komet 5 program (Kinetic, UK). The statistical analysis of mean values was carried out with the Mann-Whitney *U* test.

2.7. Cytotoxicity assay

A Cell Counting Kit-8 (CCK-8) assay kit Sigma-Aldrich was used to evaluate the toxicity of the different treatments in the cells. The cells were dispersed into a 96-well plate and after 24 h the compounds were added as described before. CCK-8 solution was then added to each well and the plate was incubated for 2 h. The absorbance was measured at 450 nm using a microplate reader. Every treatment at every concentration was done in triplicate and the cytotoxicity results are given as the mean with the error bars corresponding to the standard deviation.

3. Results

3.1. Core size in water and in cell growing media

TEM images of the FeONPs used for this work are collected in Fig. 1 corresponding to the NPs solubilized in water (A) and also in the cell growing media (B) (depleted in Fe). The sphere-like structures can be seen in both cases corresponding to the iron hydroxides cores. The measurement of the core diameter resulted in 4.0 ± 0.6 nm for the sucrose coated FeONPs and 7.5 ± 1.2 nm for the ferritin encapsulated FeONPs solubilized in water. The solubilization of the sucrose coated FeONPs in the cell growing media produced an interaction between the particles (probably ascribed to dipolar interactions) that resulted in NPs aggregation. As illustrated in Fig. 1B (left column), small clusters of about 5–8 nanoparticles (8-20 nm) and large agglomerates up to 200 nm (see pointing arrows in the Fig. 1B) were observed by TEM (also by DLS, data not shown). Such effect was not observed in the ferritin encapsulated NPs.

3.2. Iron uptake by Caco-2 and HT-29 cell lines

Cells were incubated with the different Fe nanocompounds and $FeSO_4$ at 100 and 500 μmol L^{-1} Fe at 37 °C during 48 h. It is important to address that special cell culture conditions were taken by using an Fe-depleted growing media and the minimum percentage of fetal

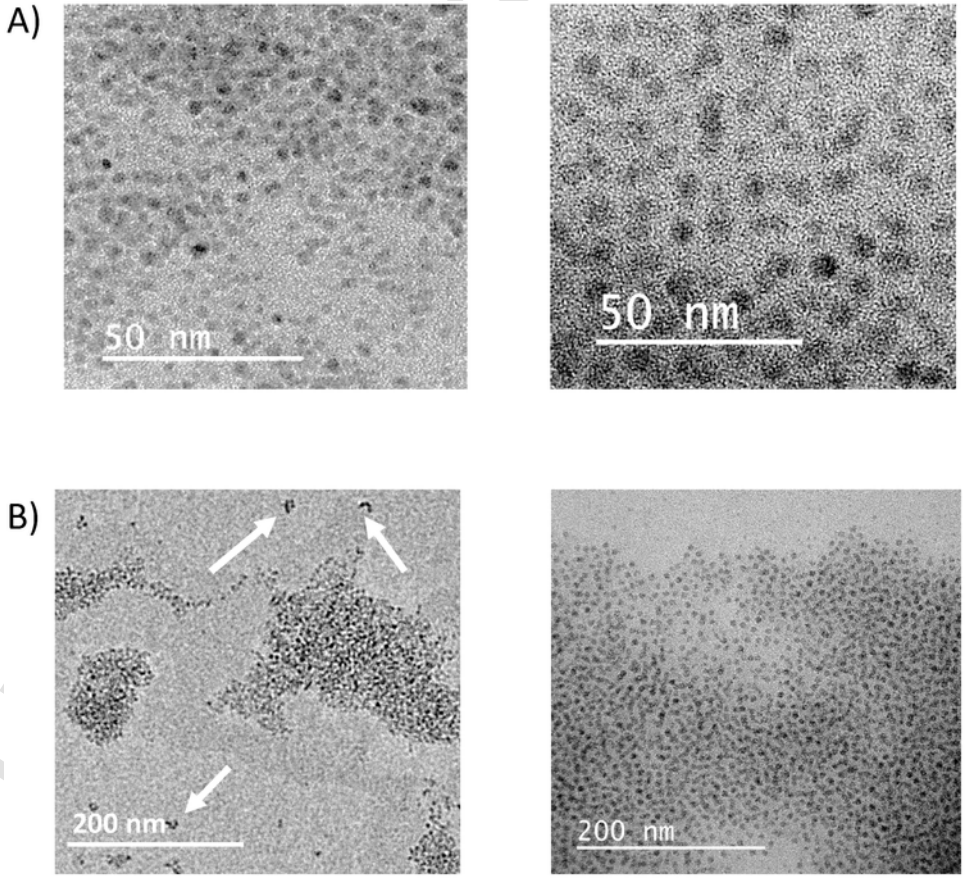

Fig. 1. TEM images of the sucrose coated FeONPs solubilized in water (A) and in the cell growing media (B). The solubilization in the cell growing media produced an interaction between the particles that resulted in NPs aggregation.

bovine serum (9%) to preserve cell viability and decrease Fe contribution other than the treatments. After cell lysis (the cell number in the case of HT-29 was 1.1×10^6 cells and 0.8×10^6 in the Caco-2, respectively) the Fe content in the lysate was measured by flow injection-ICP-MS and the results are plotted in Fig. 2 (A and B for HT-29 and Caco-2 cell lines, respectively). As can be observed, FeONPs coated with sucrose provided highest uptake in both cellular models and at both assayed concentrations followed by the ferritin encapsulated Fe. Both treatments were more efficiently incorporated than the ionic form of Fe and the uptake increased almost linearly with increasing exposure concentrations, in particular in the HT-29 cell model. However, higher uptake was observed in all cases in the Caco-2 model.

3.3. Cytosolic speciation

In addition to the total iron concentration, Fe cytosolic distribution studies were conducted by coupling size exclusion chromatography to UV–VIS and ICP-MS detection. Fig. 3 shows the Fe chromatographic profiles obtained for the cytosol of HT-29 cell line (similar results were obtained in the case of Caco-2). The inset corresponds to the TEM figure of the sucrose FeONPs treated HT-29 cells. The two main Fe-containing species eluted in the chromatograms at 11 and 15 min, respectively. Depending on the source of Fe used, a different distribution was observed among these two species. The peak eluting at 15 min corresponds to the retention time of the ferritin standard and this species showed increasing intensity upon exposure to sulfate < venofer < ferritin (Fe column recovery on each injection was > 90%). However, since the Fe stoichiometry in ferritin is variable (can vary from 200 to 4500 Fe atoms per molecule of ferritin) and ICP-MS provides just elemental information, it was not possible to directly address whether the ferritin concentration was increased upon exposure or the Fe-load into the ferritin did it. Therefore, complementary immunochemical experiments to determine, specifically, the ferritin concentration had to be conducted and are shown in the following section.

Regarding the species eluting at about 11 min, it corresponds to species of large molecular weight (> 600 kDa). In the case of the cells treated with ferritin, this species is ascribed to the formation of oligomers of ferritin, as reported by other authors that can occur when the protein is isolated [20]. In the case of the cells exposed to the NPs, this peak corresponds to the presence of nanoparticles (either isolated or aggregated) as confirmed by the injection of Venofer directly in this column (see Supplementary material).

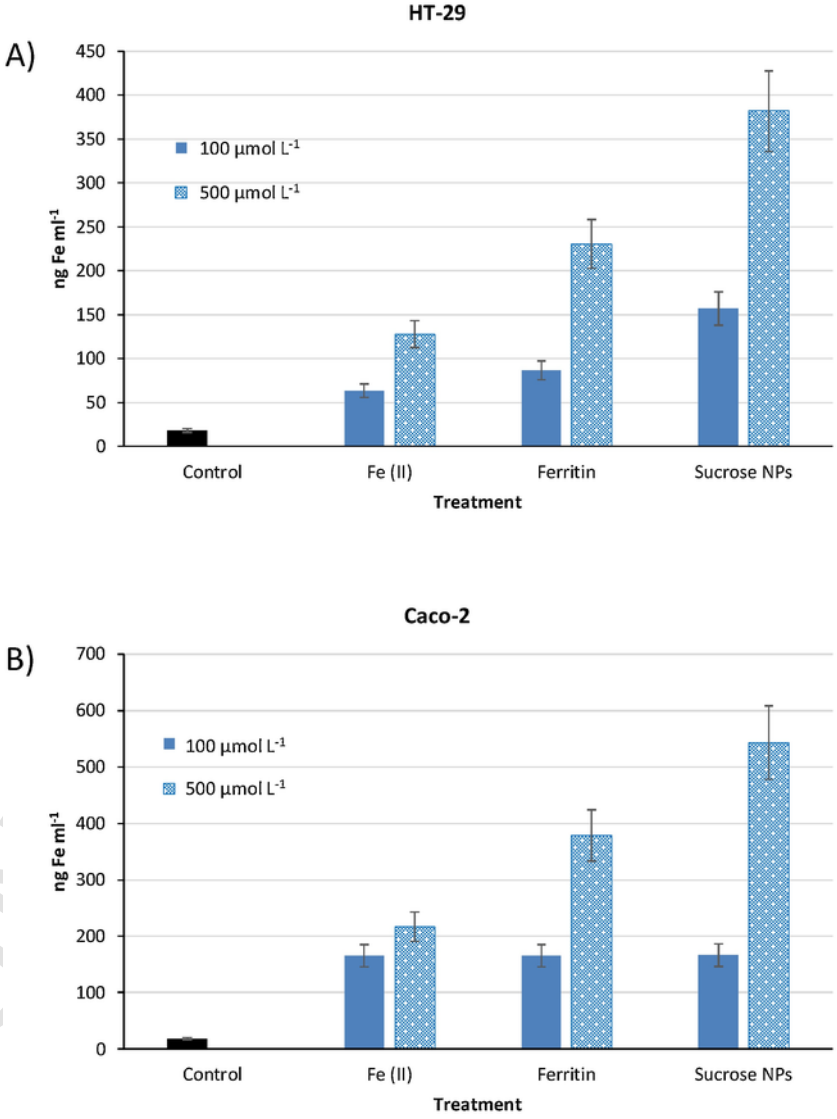

Fig. 2. Fe incorporation in both cellular models, HT-29 (A) and Caco-2 cells (B), for each Fe compound (n = 3 independent cell cultures respectively). FeONPs coated with sucrose provided highest uptake in both cellular models and at both assayed concentrations followed by the ferritin encapsulated FeONPs.

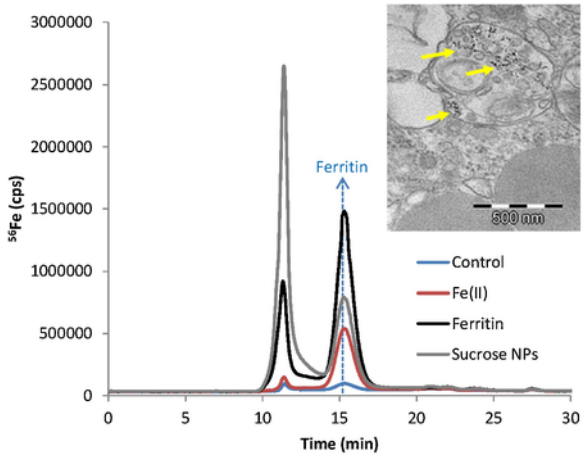

Fig. 3. Fe chromatographic profiles obtained by SEC-ICP-MS for the cytosol of HT-29 cell line. The retention time of the ferritin standard corresponds to 15 min. The inset shows the TEM picture of the cell cytosol incubated with FeONPs.

3.4. Ferritin quantitative analysis

Ferritin concentration was obtained by using a previously developed ICP-MS linked immunoassay based on a sandwich experiment with a Ru-labelled antibody [16]. The obtained results are shown in Fig. 4 for the HT-29 cell line, where the concentration (ng mL^{-1}) of the protein in the lysate is shown for every treatment. There are not a significant differences between control and sulfate treated cells regarding ferritin concentration and slightly lower values are obtained for the cells exposed to sucrose coated FeONPs. However, the only significant increment is observed when the cells are directly exposed to ferritin as nanocompound pointing out that this species is incorporated into the cell cytosol directly through the specific ferritin receptors.

3.5. Cellular cytoxicity and DNA damage

Since Fe is a potent redox compound through Fenton reaction, it is important to take into account that high Fe uptake might be associated to an increase in reactive oxygen species (ROS) formation and therefore, higher cellular toxicity. In fact, recent reports reveal that nanoparticle-induced modulation of iron and ROS levels within cancer cells and the tumor microenvironment could provide a new strategy for cancer treatment [21]. For this aim, cell viability was evaluated at different concentrations of the three species using the cell counting kit (CCK-8)

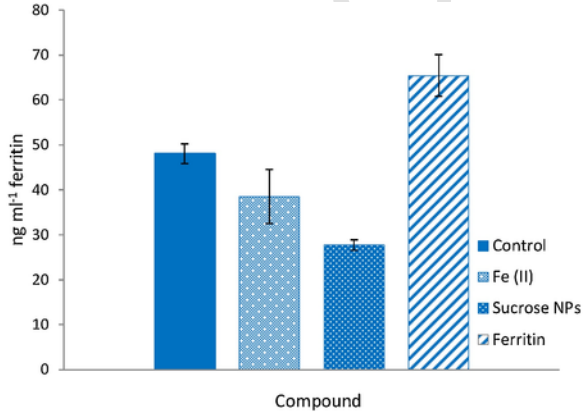

Fig. 4. Ferritin concentration obtained in the HT-29 cells treated with the three Fe-containing compounds (500 μM as Fe) and measured using an ICP-MS based sandwich immunoassay [16].

which has proved to be more sensitive than other assay like MTT, etc. The results are plotted in Fig. 5 for HT-29 and Caco-2, respectively.

In both cases, highest descent in cell viability is observed in cells exposed to FeONPs coated with sucrose which diminished cell viability to 75% at 1000 μmol L^{-1} Fe. Thus, a potent redox effect at these concentrations and with this time of exposure can be ruled out. However, first tests in order to address initial genotoxicity originated by free radicals produced during Fe metabolism were conducted by the Comet assay and using cells treated with H_2O_2 as positive control. Although both cell models proved to be suitable for this assay, Caco-2 turned out to be more sensitive to manipulation and prone to DNA unspecific degradation. Therefore, the results presented here refer to the HT-29 cell line. Fig. 6A shows the electropherograms corresponding to the control cells, cells exposed to FeONPs coated with sucrose as well as the positive control of cells treated with H_2O_2. In this case, it was possible to observe a partial DNA degradation in the treatment with FeONPs that provided a tail percentage of about 25% (Fig. 6B), which was significantly different from the other treatments and from the control cells. Thus, initial DNA damage seems to be occurring during cells exposure to this compound that is not detectable in the case of the ferritin or Fe(II) exposed cells.

4. Discussion

The two main mechanism of internalization of Fe-NPs in cells are compared in this work: through specific receptors (ferritin) and by "unspecific" endocytosis (sucrose coated FeONPs). In addition, both mechanisms are compared with the uptake of Fe(II) salts (most conventional formulation for iron supplementation) in two enterocyte-like cell models. Since NPs uptake and biological function depends not only on the surface charge but also on the shape and size, it is important to consider the effect of the cell growing medium on the studied NPs. The first observation was the partial aggregation of the sucrose FeONPs once solubilized in the cell growing media (which was not observed in the ferritin NPs). This is probably ascribed to the presence of the components of the incubation medium (e.g. proteins) that induce electrostatic interaction of the NPs. Such interaction has been also reported to help decreasing cytotoxicity for many NPs but results in a significant

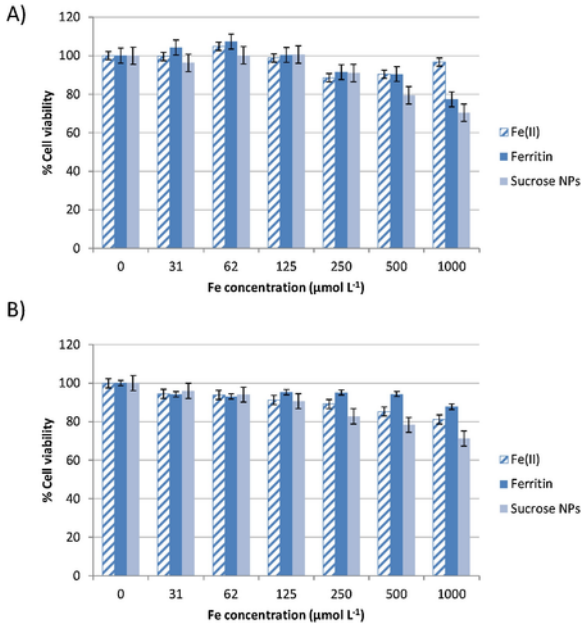

Fig. 5. Cell viability results using the CCK-8 kit for HT-29 (A) and Caco-2 cells (B), at different concentrations of the three species. Highest descent in cell viability is observed in cells exposed to FeONPs coated with sucrose.

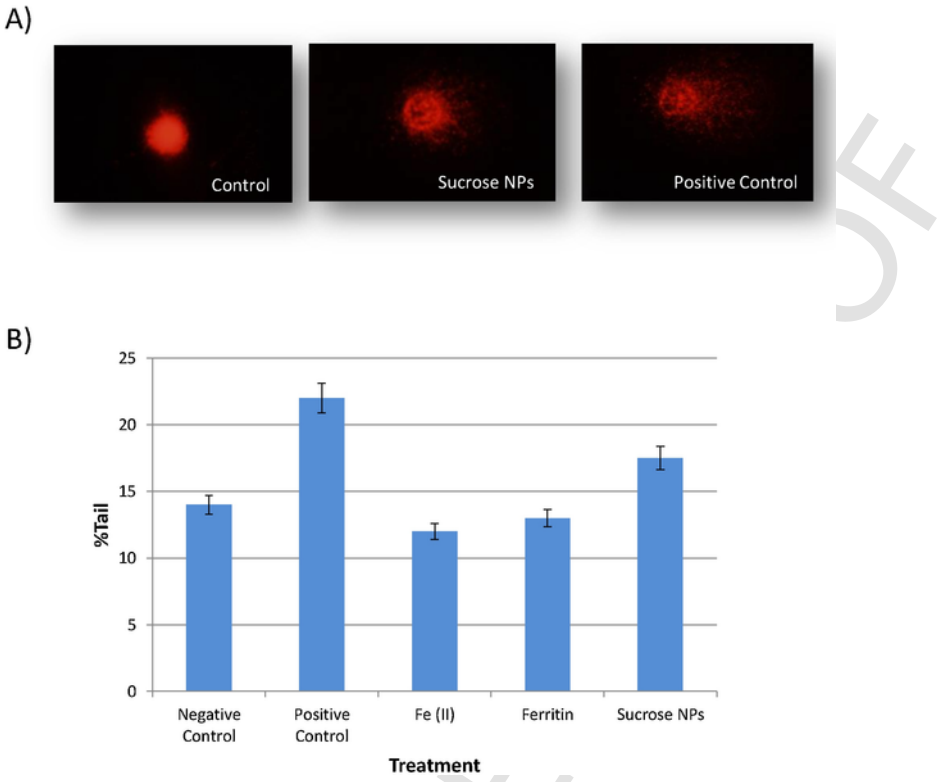

Fig. 6. Electropherograms corresponding to the control cells, cells exposed to FeONPs coated with sucrose as well as the positive control of cells treated with H_2O_2(A). It is observed a partial DNA degradation in the treatment with FeONPs that provides a tail percentage of about 25% (B), the highest in comparison with the others treatments.

change in their mean size (moving from individual NPs with a core size of 4 ± 1 nm to aggregates up to 200 nm) [22]. However, since enterocytes have shown to preferentially ingest particles in the range between 100 and 200 nm, aggregation does not represent an issue regarding uptake, in this case, and might be even advantageous with respect to the use of smaller NPs [23].

Iron uptake experiments in the two cell models by ICP-MS revealed highest Fe incorporation in the case of the sucrose coated FeONPs. Values of about 0.14 pg Fe per cell in the cells exposed to 100 $\mu mol\,L^{-1}$ Fe and 0.35 pg Fe per cell in the cells exposed to 500 $\mu mol\,L^{-1}$ in the HT-29 were obtained. These values are, as average, 1.7-fold higher than those obtained when using ferritin as nanoparticulated formulation and about 3-fold higher than in the case of Fe (II). In addition, the Caco-2 model shows higher uptake for all the compounds when compared to HT-29 but the relative differences among treatments are consistent in both cell models, in particular at the higher doses. Out of these results it can be extracted that unspecific NPs endocytosis is prevalent to the uptake through specific receptors (either using DMT1 as for Fe(II) or ferritin specific receptors). Comparing ferritin and Fe(II), it has been documented that ferritin uptake at higher concentrations can be also driven by endocytosis and this can serve as the explanation for the similar uptake values observed for Fe(II) and ferritin at low concentrations (100 $\mu mol\,L^{-1}$) and the differences found at higher doses (500 $\mu mol\,L^{-1}$) in both cell models. In addition, the endocytosis of the FeONPs seems to occur directly from the nanoparticulated form and TEM figures permits to detect, clearly, the presence of these NPs (both, dispersed and aggregated) in the cytosol of both cell models.

The fractionation of the incorporated Fe in the cytosol of the treated cells was conducted using SEC-ICP-MS. The results of Fig. 3 (SEC-ICP-MS) revealed that ferritin is the main Fe containing protein within the cell cytosol and the absolute protein concentration is reported in Fig. 4. Since ferritin can allocate a variable concentration of Fe within the protein cage (up to 4500 atoms of Fe per molecule of ferritin), the cellular uptake of Fe(II) as sulfate produced a significant increase of the stored Fe within the existing cytosolic ferritin and an increase in the Fe profile. In addition, the ferritin treated cells uptake and accumulate this protein by increasing the measured intracellular ferritin concentration in respect to the control and, subsequently, the Fe signal in the SEC-ICP-MS. Finally, the results of the treatment with NPs, which showed slightly lower protein concentration but higher Fe signal by SEC-ICP-MS, reveal that the Fe loading of ferritin is increased upon exposure to these FeONPs.

Such increase could be ascribed to the release of Fe(III) due to the partial degradation of the NPs that could be further reduced to Fe(II) and be incorporated into the existing cytosolic ferritin. In addition, another fraction of the FeONPs can be directly endocyted and stored by the enterocytes providing an intense Fe peak at the void volume of the chromatography (see Fig. 4). This conclusion was extracted from the fact that a similar chromatographic profile was obtained when the sucrose coated FeONPs were directly injected into the system (see Supplementary information). However, the two experiments (SEC-ICP-MS and ferritin analysis) are necessary and complementary to obtain these conclusions.

Negligible cellular toxicity, even taking into account the high Fe uptake (up to 2% in the case of the sucrose coated FeONPs) was been detected in all the evaluated treatments and cell models. Just concentrations above 500 $\mu mol\,L^{-1}$ provided a viability decrease above 20% (see Fig. 5). However, the number of oxidative DNA modifications induced by reactive species arising from iron-driven reactions is high, according to the literature [24]. The degree of genotoxic damage in an individual cell can be easily measured with the comet assay which is, in principle, simple and inexpensive to perform but is also very sensitive. With this assay we it is possible to show, not only the indirect formation of ROS, but the effect of ROS on the DNA damage (one of the most biomarkers usually chosen to measure the effects of ROS in cells) that can be detected even when not detectable cytotoxicity is observed. The evalua-

tion of the DNA induced toxicity (more sensitive) through the Comet assay revealed a significant DNA damage in the doses of 500 μmol L^{-1} for the sucrose coated FeONPs, which is probably related to the higher uptake of this nanocompound in the HT-29 cell model. Such result is not surprising since iron is a potent redox element that might undergo (bio)chemical oxidation/reduction within cells. In this case, a reduction has occurred (since the uptake of Fe by ferritin occurs only with Fe(II) and the sucrose coated FeONPs contain Fe(III)) and thus, the generation of free radicals within the cell cytosol is almost ensured.

5. Conclusions

This study has confirmed that although higher Fe uptake has been observed when using negatively charged sucrose coated FeONPs, the most efficiently Fe storage (in a biologically compatible form) is in the form of ferritin NPs. The sucrose coated FeONPs provide a high level of intracellular nanoparticulated Fe that could be further converted into ionic Fe species. Since Fe is a potent redox element, the consequences of such release would need to be stablished and initial DNA damage has been observed. On the other hand, the administration of Fe-ferritin incorporates Fe in cells in a more efficient manner than Fe(II) salts and does not yield any detectable toxicity effects to cells.

Declarations of interest

None.

Acknowledgments

The authors want to acknowledge the help of Dr. L. M. Sierra with the Comet experiments, C. Sanchez from University of Granada for the TEM experiments and the Ministry of Economy and Competitiveness for the support through the project MINECO-2017 CTQ2016-80069-C2-1R. D. Turiel wants to acknowledge also his grant from the Spanish Ministry of Education and Science for the FPU grant FPU15/02415.

References

[1] B.G. Danielson, J. Am. Soc. Nephrol. 15 (2004) S93–S98.
[2] M. Muñoz, J.A. García-Erce, A.F. Remacha, J. Clin. Pathol. 64 (2011) 287–296.
[3] A. Dostal, C. Chassard, F.M. Hilty, M.B. Zimmermann, T. Jaeggi, S. Rossi, C. Lacroix, J. Nutr. 142 (2012) 271–277.
[4] D. Moretti, M.B. Zimmermann, R. Wegmuller, T. Walczyk, C. Zeder, R.F. Hurrel, Am. J. Clin. Nutr. 83 (2006) 632–638.
[5] D.I.A. Pereira, S.F.A. Bruggraber, N. Faria, L.K. Poots, M.A. Tagmount, M.F. Aslam, D.M. Frazer, C.D. Vulpe, G.J. Anderson, J.J. Powel, Nanomedicine 10 (2014) 1877–1886.
[6] F.M. Hilty, M. Arnold, M. Hilbe, A. Teleki, J.Y.N. Knijnenburg, F. Ehrensperger, R.F. Hurrel, S.E. Pratsinis, W. Langhans, M.B. Zimmerman, Nat. Nanotechnol. 5 (2010) 374–380.
[7] M.R. Jahn, H.B. Andreasen, S. Fütterer, T. Nawroth, V. Schünemann, U. Kolb, W. Hofmeister, M. Muñoz, K. Bock, M. Meldal, P. Langguth, Eur. J. Pharm. Biopharm. 78 (2011) 480–491.
[8] A.K. Gupta, M. Gupta, Biomaterials 26 (2005) 3995–4021.
[9] R. Yang, Z. Zhou, G. Sun, Y. Gao, J. Xu, Trends Food Sci. Technol. 44 (2015) 189–200.
[10] I. Murgia, P. Arosio, D. Tarantino, C. Soave, Trends Plant Sci. 17 (2012) 47–55.
[11] S. Kalgaonkar, B. Lönnerdal, J. Nutr. Biochem. 20 (2009) 304–311.
[12] C.D. San Martin, C. Garri, F. Pizarro, T. Walter, E.C. Theil, M.T. Núñez, J. Nutr. 138 (2008) 659–666.
[13] J.Y. Li, N. Paragas, R.M. Ned, A. Qiu, M. Viltard, T. Leete, I.R. Drexler, X. Chen, S. Sanna-Cherchi, F. Mohammed, D. William, C. Sheng Lin, K.M. Schmidt-Ott, N.C. Andrews, J. Barasch, Dev. Cell 16 (2009) 35–46.
[14] D.L.J. Thorek, A. Tsourkas, Biomaterials 29 (2008) 3583–3590.
[15] V.S. Kalambur, E.K. Longmire, J.C. Bischof, Langmuir 23 (2007) 12329–12336.
[16] M. Muñoz, S. Gómez-Ramírez, E. Martín-Montañez, J. Pavía, J. Cuenca, J.A. García-Erce, Nutr. Hosp. 27 (2012) 1817–1836.
[17] M. Corte, M. Espina, L.M. Sierra, E. Blanco, T. Ames, M. Montes-Bayón, A. Sanz-Medel, Biochem. Pharmacol. 98 (2015) 69–77.
[18] T. Konz, E. Añón, M. Montes-Bayón, A. Sanz-Medel, Anal. Chem. 85 (2013) 8334–8340.
[19] D. García Sar, M. Montes-Bayón, L. Aguado Ortiz, L.M. Sierra Zapico, E. Blanco González, A. Sanz-Medel, Anal. Bioanal. Chem. 390 (2008) 37–44.
[20] T. Konz, M. Montes-Bayón, A. Sanz-Medel, Analyst 139 (2014) 5451.
[21] S. Zanganeh, G. Hutter, R. Spitler, O. Lenkov, M. Mahmoudi, A. Shaw, J.S. Pajarinen, H. Nejadnik, S. Goodman, M. Moseley, L.M. Coussens, H.E. Daldrup-Link, Nat. Nanotechnol 11 (2016) 986–994.
[22] A. Petri-Fink, B. Steitz, A. Finka, J. Salaklang, H. Hofmann, Eur. J. Pharm. Biopharm. 68 (2008) 129–137.
[23] K.Y. Win, S.S. Feng, Biomaterials 26 (2005) 2713–2722.
[24] M. Krucewski, Mut. Res. Fund. Mol. Mech. Mut. 531 (2008) 81–92.